Solvable random network model for disordered sphere packing

Souvik Dhara, Johan S.H. van Leeuwaarden, and Debankur Mukherjee
Eindhoven University of Technology, Department of Mathematics and Computer Science, P.O. Box 513, 5600 MB Eindhoven, The Netherlands

A notorious problem in physics is to create a solvable model for random sequential adsorption of non-overlapping congruent spheres in the d-dimensional Euclidean space with $d \geq 2$. Spheres arrive sequentially at uniformly chosen locations in space and are accepted only when there is no overlap with previously deposited spheres. Due to spatial correlations, characterizing the fraction of accepted spheres or the area covered by the deposited spheres remains largely intractable. We study these disordered sphere packings by taking a radically novel approach that compares random sequential adsorption in Euclidean space to the nearest-neighbor blocking on a sequence of clustered random networks with a growing number of vertices. This tractable network model leads to a precise characterization of the coverage and elementary laws that describe the packing fraction as a function of density and dimension. By investigating the spatial dimensions two to five over wide density ranges, we show that these laws are accurate and universal. The model also supports a previously conjectured lower bound on the densest packing in high dimensions.

PACS numbers: 02.50.Ga, 68.43.-h, 89.75.-k

arXiv:1611.05019v1 [math.PR] 15 Nov 2016

The packing of congruent spheres in the d-dimensional Euclidean space has been a topic of great interest across the sciences, serving as basic models in condensed matter and quantum physics [1–4], nanotechnology [5, 6], information theory and optimization problems [7–9]. A huge body of mathematical literature [10–16] is devoted to the rigorous understanding of the largest possible fraction of the space covered by the spheres in dimensions $3, 8, 24$; the problem in general dimensions remains open. Although the densest packings are generally believed to be ordered (regular lattices or crystal structures), disordered packings can serve as approximations (lower bounds). In fact, there are reasons to believe that in sufficiently high dimension, the densest packing tends to become disordered rather than ordered, which hints at the existence of disordered classical ground states for some continuous potentials [17, 18]. Having almost no analytical result in high dimensions, this strongly motivates the study of disordered packings. Disordered sphere packings also turn up naturally in numerous experimental and real-world settings, ranging from the deposition of nano-scale particles on polymer surfaces, adsorption of proteins on solid surfaces to the creation of logic gates for quantum computing, and many more applications in domains as diverse biology, ecology and sociology, see [19–21] for extensive surveys.

Disordered random packings in continuum spaces are notoriously hard to analyze, because particles display strong local and global spatial correlations. These correlations can be understood by viewing the packing as a dynamic process referred to as random sequential adsorption (RSA) [19, 21]. At each time epoch, a center appears at a uniformly chosen location in space, and an attempt is made to place a sphere with the chosen point as its center. The new sphere must either fit in the empty area allowed by the hard-core exclusion interaction with the spheres deposited earlier, or its deposition attempt is discarded. Of particular interest is the proportion of accepted spheres, or equivalently, the volume covered by the accepted spheres. Fig. 1 illustrates three instances of this RSA process in 2D.

The precise setting in this paper considers packing in a finite-volume box $[0,1]^d$, filled with 'small' spheres of radius r and volume $V_d(r)$. We will make use of the fact that this RSA process of spheres in the continuum can equivalently be viewed as RSA of particles on the vertices of a spatial random network with nearest-neighbor blocking. The n attempted locations in $[0,1]^d$ of centers are regarded as the vertices of the network and two vertices are connected if they are at most $2r$ distance apart. The interaction network, thus obtained, is known as the random geometric graph (RGG). Since the volume of $[0,1]^d$ is 1, the probability that two randomly chosen vertices are connected is equal to the volume of a sphere of radius $2r$, given by

$$V_d(2r) = \frac{\pi^{d/2}(2r)^d}{\Gamma(1+d/2)} \tag{1}$$

and the average degree of a vertex is $c = nV_d(2r)$. Since c is the average number of overlaps per sphere, with all other attempted spheres, we interchangeably use the terms density and average degree for c. To maintain a constant density c in the large-network limit, as $n \to \infty$, the spheres need to become smaller when more vertices are added to the graph, and the radius should scale as a function of n according to

$$r = \frac{1}{2}\left[\frac{c\Gamma(1+d/2)}{n\pi^{d/2}}\right]^{1/d}. \tag{2}$$

Notice that it is equivalent to consider the deposition of spheres with fixed radii into a box of growing volume. We parameterize the RGG model by the density c and the dimension d, and henceforth write this as $\mathrm{RGG}(c,d)$. A typical instance of $\mathrm{RGG}(5,2)$ with $n = 1000$ vertices is shown in Fig. 2. Random sequential adsorption on a

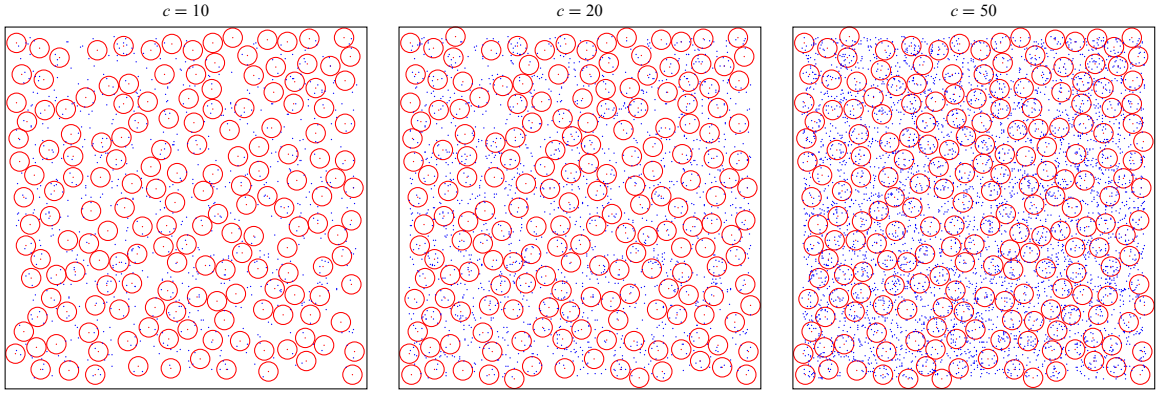

FIG. 1. Random sequential adsorption in 2D with an increasing number of deposition attempts. Dots indicate the centers of accepted (red) and discarded (blue) spheres. The average number of overlaps per sphere with all other attempted spheres is referred to as the density c.

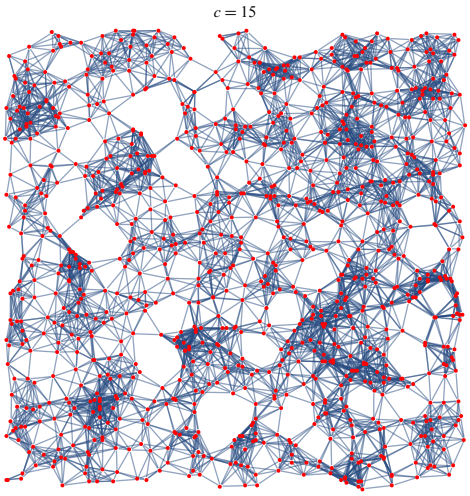

FIG. 2. RGG$(15, 2)$ graph with 1000 vertices: two vertices share an edge if they are less than $2r$ distance apart, where r is such that a vertex has on average $c = 15$ neighbors. Notice the many local clusters.

graph selects vertices uniformly at random and activates them if none of the neighbors are active. For RSA in the continuum, notice that any two centers of the deposited spheres are at least $2r$ distance apart, and therefore the RGG model with radius $2r$ and nearest-neighbor blocking corresponds to the deposition of non-overlapping spheres of radius r. The number of deposited spheres after n attempts in the continuum RSA has the same law as the number of active vertices for RSA on RGG(c, d) with n vertices. Let $J_n(c, d)$ be the fraction of active vertices in the RGG(c, d) model on n vertices. Since each sphere covers a region of volume $V_d(r)$, the total volume covered by the accepted spheres is $J_n(c, d) \times n \times V_d(r)$. Further, $c = nV_d(2r)$ and $V_d(2r) = 2^d V_d(r)$, so that the total volume covered is

$$J_n(c, d) \times \frac{c}{2^d}. \tag{3}$$

Thus the problems of determining the total volume covered by the deposited spheres in $[0, 1]^d$, and determining the fraction of active vertices in the RGG(c, d) model, are equivalent. That is why we will henceforth focus only on the quantity $J_n(c, d)$. While it was proved in [22] that the limit $J_n(c, d) \to J(c, d)$ exists, no quantitative characterization of $J(c, d)$ for dimensions ≥ 2 has been provided till date, and so far the main methods to study this problem rely on extensive simulations [23–29]. We propose a novel approach that considers RSA on a clustered random graph model. This random network will be designed to match the local spatial properties of the RGG model in terms of density and clustering, but remains amenable to rigorous mathematical treatment including the limiting packing fraction.

Random graphs serve to model large networked systems, but are typically unfit for capturing local clustering in the form of relatively many short cycles. This can be resolved by locally adding so-called households or small dense graphs [30–36]. Vertices in a household have a much denser connectivity to all (or many) other household members, which enforces local clustering. We now introduce a new household model, called clustered random graph model (CRG), designed for the purpose of analyzing the disordered packing problem. An arbitrary vertex in the CRG model has local or short-distance connections with nearby vertices, and global or long-distance connections with the other vertices. When pairing vertices, the local and global connections are formed according to different statistical rules. The degree distribution of a typical vertex is taken to be Poisson(c) (approximately) in both the RGG and CRG model. In the CRG(c, α) model however, the total mass of connectivity measured in the density parameter c, is split into αc to account for direct local blocking and $(1 - \alpha)c$ to incor-

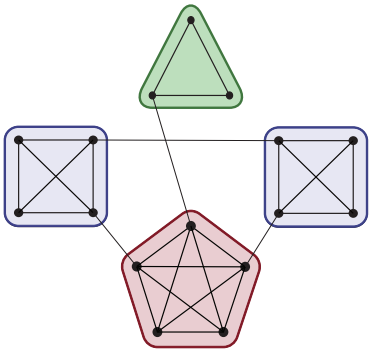

FIG. 3. Example topology generated by the CRG(c, α) model.

porate the propagation of spatial correlations over longer distances. The CRG(c, α) model with n vertices is then defined as follows (see Fig. 3):

- Partition the n vertices into random households of size $1 + \text{Poisson}(\alpha c)$. This can be done by sequentially selecting $1 + \text{Poisson}(\alpha c)$ vertices uniformly at random and declaring them as a household, and repeat this procedure until at some point the next $1+\text{Poisson}(\alpha c)$ random variable is at most the number of remaining vertices. All the remaining vertices are then declared a household too, and the household formation process is completed.

- Now that all vertices are declared members of some household, the random graph is constructed according to a local and a global rule. The local rule says that all vertices in the same household get connected by an edge, leading to complete graphs of size $1+\text{Poisson}(\alpha c)$. The global rule adds a connection between any two vertices belonging to two different households with probability $(1 - \alpha)c/n$.

This creates a class of random networks with a fixed density c and tunable level of clustering via the free parameter α. With the goal to design a solvable model for the random packing process, the CRG(c, α) model has $nc/2$ connections to build a random structure that mimics the local spatial structure of the RGG(c, d) model on n vertices.

Seen as the topology underlying the random packing problem, the CRG(c, α) model incorporates local clusters of overlapping spheres, which occur naturally in random geometric graphs; see Fig. 2. We can now also consider RSA on the CRG(c, α) model, by using the greedy algorithm that constructs an independent set on the graph by sequentially selecting vertices uniformly at random, and placing them in the independent set unless they are adjacent to some vertex already chosen. The packing fraction $\hat{J}_n(c, \alpha)$ is then the fraction of activated vertices in the CRG(c, α) model, hence the size of the independent set divided by the network size n. From a high-level perspective, we will solve the RSA problem on the CRG(c, α) model, and translate this solution into an equivalent result for RSA on the RGG(c, d). Our ansatz is that for large enough n, a unique relation can be established between $d \longleftrightarrow \alpha = \alpha_d$, so that the jamming constants are comparable, i.e.,

$$J_n(c, d) \approx \hat{J}_n(c, \alpha_d), \tag{4}$$

and virtually indistinguishable in the large network limit.

In order to do so, we map the CRG(c, α) model onto the RGG(c, d) model by imposing two natural conditions. The first condition matches the average degrees in both topologies, i.e., c is chosen to be equal to $nV_d(2r)$. The second condition tunes the local clustering. Let us first describe the clustering in the RGG model. Consider two points chosen uniformly at random in a d-dimensional hypersphere of radius $2r$. Then what is the probability that these two points are themselves at most $2r$ distance apart? From the RGG perspective, this corresponds to the probability that, conditional on two vertices u and v being neighbors, a uniformly chosen neighbor w of u is also a neighbor of v, which is known as the local clustering coefficient [37]. In the CRG(c, α) model, on the other hand, the relevant measure of clustering is α, the probability that a randomly chosen neighbor is a neighbor of one of its household members. We then choose the unique α-value that equate to the clustering coefficient of RGG. Denote this unique value by α_d, to express its dependence on the dimension d. In order to obtain an explicit characterization for α_d, let $B(\boldsymbol{x}, 2r)$ denote the d-dimensional sphere with radius $2r$, centered at $\boldsymbol{x} \in \mathbb{R}^d$, and $V_d(2r)$, its volume. Pick any point $\boldsymbol{V}$ uniformly at random from $B(\boldsymbol{x}, 2r)$. Write $u \leftrightarrow v$ to say that u and v share an edge. The above reasoning gives

$$\begin{aligned}
\alpha_d &= \frac{\mathbb{P}\left(u \leftrightarrow v, u \leftrightarrow w, v \leftrightarrow w\right)}{\mathbb{P}\left(u \leftrightarrow v, u \leftrightarrow w\right)} \\
&= \frac{1}{(V_d(2r))^2} \int_{B_d(\mathbf{0}, 2r)} \mathbb{P}\big(\boldsymbol{w} \in B_d(\mathbf{0}, 2r) \cap B_d(\boldsymbol{v}, 2r)\big) \mathrm{d}\boldsymbol{v} \\
&= \frac{1}{V_d(2r)} \mathbb{E}[|B_d(\mathbf{0}, 2r) \cap B_d(\boldsymbol{V}, 2r)|].
\end{aligned} \tag{5}$$

The expected value in (5) can be calculated explicitly (see Appendix C), which gives

$$\alpha_d = d \int_0^1 x^{d-1} I_{1-\frac{x^2}{4}}\Big(\frac{d+1}{2}, \frac{1}{2}\Big) \mathrm{d}x, \tag{6}$$

where $I_z(a, b)$ is the normalized incomplete beta integral

$$I_z(a, b) = \frac{\int_0^z x^{a-1}(1-x)^{b-1} \mathrm{d}x}{\int_0^1 x^{a-1}(1-x)^{b-1} \mathrm{d}x}. \tag{7}$$

Table I shows the numerical values of α_d in dimensions 1 to 5. With the uniquely characterized α_d in (6), the CRG(c, α_d) model can now serve as a generator of random topologies for guiding the RSA process.

In contrast to the Euclidean space, the packing of the CRG(c, α_d) model through RSA is analytically solvable,

d	1	2	3	4	5
α_d	0.750000	0.586503	0.468750	0.379755	0.310547

TABLE I. Numerical values for α_d for dimensions 1 to 5.

even at later times when the filled space becomes more dense (c is large) and the deposition events become more correlated. To solve this problem, we will extend the mean-field techniques recently developed for analyzing RSA on random graph models [38–41]. The main goal of these works was to find greedy independent sets (or colorings) of large random networks. All these results, however, were obtained for non-geometric random graphs, typically used as first approximations for sparse interaction networks in the absence of any known geometry.

We now consider the CRG(c, α) model, and introduce an algorithm that sequentially activates the vertices and explores the graph while obeying the hard-core exclusion constraint (see Appendix A for further details). Asymptotic analysis of the algorithm in the large-graph limit $n \to \infty$ then leads to explicit characterizations of the packing fraction. The algorithm carries along three types of vertices: active, frozen and neutral. Initially, all the vertices are neutral; at each step a neutral vertex is selected uniformly at random and declared active. This in turn causes some vertices (the neighbors which are still neutral) to become frozen. The neighbors of the newly active vertex are selected as follows: a number Poisson(αc) of vertices are selected uniformly at random from the set of all vertices that do not yet belong to any household, and together form the household of the activated vertex. It is possible that some of these selected vertices are already frozen due to distant connections with a vertex outside its household that was activated earlier. Then the newly activated vertex connects to any other neutral vertex with probability $(1-\alpha)c/n$, which creates its distant neighbors. These vertices belong to a different household, but are frozen nevertheless. For the CRG(c, α) model on n vertices, recall that $\hat{J}_n(c, \alpha)$ denotes the packing fraction of active vertices. We then have the following result.

Theorem 1. *For any $c > 0$ and $\alpha \in [0, 1]$, as $n \to \infty$, $\hat{J}_n(c, \alpha) \xrightarrow{\mathbb{P}} \hat{J}(c, \alpha)$, where $\hat{J}(c, \alpha)$ is the smallest nonnegative root of the deterministic function $x(t)$ described by the integral equation*

$$x(t) = 1 - t - \int_0^t \left(\frac{x(s)\alpha c}{1 - (\alpha c + 1)s} + (1-\alpha)cx(s) \right) \mathrm{d}s. \tag{8}$$

In particular, as $c \to \infty$,

$$\hat{J}(c, \alpha_d) \sim \frac{1}{1 + \alpha_d c}. \tag{9}$$

The ODE (8) can be understood intuitively. Rescale time by n, so that after rescaling the algorithm has to end before time $t = 1$ (because the network size is n). Now think of $x(t)$ as the fraction of neutral vertices at time t. Then clearly $x(0) = 1$, and the drift $-t$ says that one vertex activates per time unit. Upon activation, a vertex blocks its αc household members and on average $(1-\alpha)c$ other vertices outside its household. At time t, the fraction of vertices that are not members of any discovered households equals on average $(1 - (1 + \alpha c)t)$ and all vertices which are not part of any discovered households, are potential household members of the newly active vertex (irrespective of whether it is blocked or not). Since household members are uniformly selected at random, only a fraction $x(t)/(1 - (1 + \alpha c)t)$ of the new αc household members will belong to the set of neutral vertices. Moreover, since all $x(t)n$ vertices are being blocked by the newly active vertex with probability $(1-\alpha)c/n$, on average $(1-\alpha)cx(t)$ neutral vertices will be blocked due to distant connections. Notice that the graph will be maximally packed when $x(t)$ becomes zero, i.e., there are no neutral vertices that can become active. This explains why $\hat{J}(c, \alpha)$ should be the smallest root of (8). The simple law (9) thus describes the packing fraction as a function of density (large) and dimension, and suggests that the fraction of vertices in the packing as a function of the density c scales as $(1 + \alpha_d c)^{-1}$.

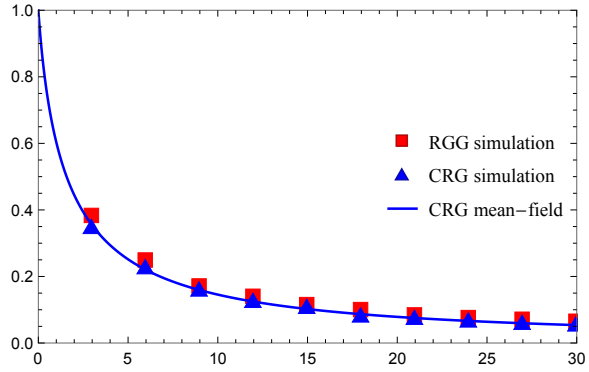

FIG. 4. Mean-field limit for CRG(c, α_2) and simulation with 1000 vertices of RGG$(c, 2)$ and CRG(c, α_2) for $0 \le c \le 30$.

A rigorous proof of Theorem 1 is presented in Appendix A, and uses martingale decomposition and functional limit theorems. Upon substituting $\alpha = \alpha_d$, $\hat{J}(c, \alpha_d) = \lim_{n\to\infty} \hat{J}_n(c, \alpha_d)$ is completely characterized by (8) and serves an approximation for the intractable counterpart $J(c, d)$, the limiting jammed fraction for the RGG(c, d) model. The choice of α_d, as discussed earlier, is given by (6) and shown in Table I. Figs. 4 and 5 validate the mean-field limit for the CRG model, and show the theoretical values $\hat{J}(c, \alpha_d)$ from Theorem 1, along with the simulated values of RSA on the RGG(c, d) model for values of c ranging from 0 to 20, $d = 3, 4, 5$, and 1000 vertices, respectively. The remarkable agreement of the $\hat{J}(c, \alpha_d)$-curve with the simulated results shows that the integral equation (8) accurately describes the mean-field large-network behavior of the packing process, not only for the CRG model, but also for the RGG model.

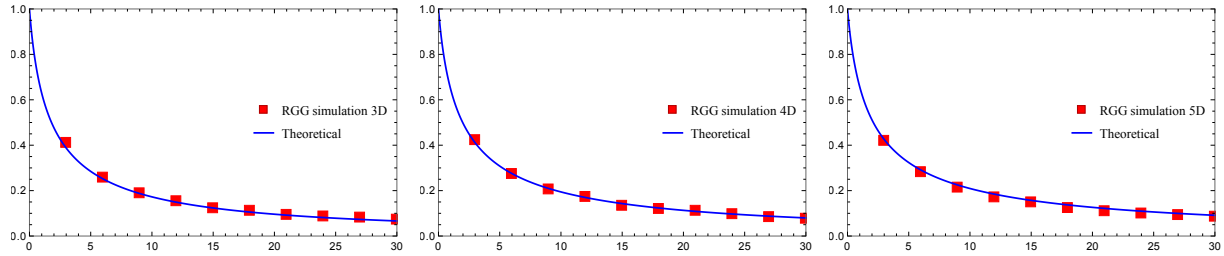

FIG. 5. Mean packing fraction according to the theoretical values $\hat{J}(c, \alpha_d)$ compared with simulation of the RGG(c, d) model for 1000 vertices, $0 \leq c \leq 20$, $d = 3, 4, 5$.

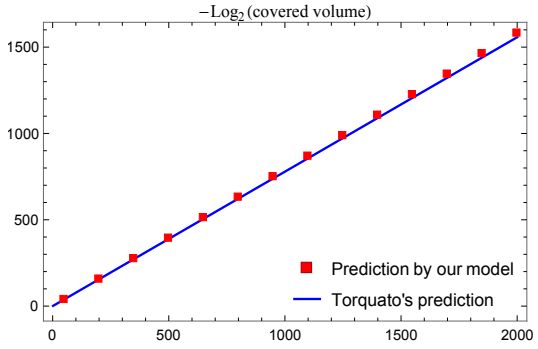

FIG. 6. $\log_2$(covering volume) is plotted as a function of dimenson. The blue line is $y = 0.77865x$ and the red dots are $y = \log_2(2^x \alpha_x)$ for increasing values of x.

Let us finally consider what happens in high dimensions. We note that $\alpha_d \to 0$ as $d \to \infty$. Thus, the interaction network described by the CRG(c, α_d) model becomes almost like the mean-field Erdős-Rényi random graph model, which supports the widely believed conjecture that in high dimensions the interaction network associated with the random geometric graph loses its local clustering property [42]. The total scaled volume $cJ(c, d)/2^d$ covered by the deposited spheres in dimension d, serves as a lower bound for the densest packing, generally believed to be ordered. Due to the accurate description provided by the CRG model, $c\hat{J}(c, \alpha_d)/2^d$ also gives a good approximation for the disordered lower-bound. Indeed, for large c, (9) yields $\hat{J}(c, \alpha_d) \sim 1/(\alpha_d c)$, and therefore, in any dimension d, our model predicts that the lower bound takes the form

$$\hat{J}(c, \alpha_d) \times \frac{c}{2^d} = \frac{1}{2^d \alpha_d}, \tag{10}$$

and $-\log_2(\text{covered volume}) = \log_2(2^d \alpha_d)$. Let us compare this with the lower bound $2^{-0.77865\ldots d}$ conjectured by Torquato and Stillinger [17]. Fig. 6 shows an almost unbelievable agreement between both predictions, and hence strongly supports the validity of the modeling approach and the discovered laws in this paper.

In summary, the CRG(c, α_d) model reduces all possible interactions among pairs of vertices to only two principal components: the local interactions due to the clustering, and a mean-field long-range interaction. While the CRG(c, α_d) model seems a rather crude approximation of the RGG(c, d) topology, it proves sufficient for the packing problem, as evidenced by Figs. 4–6. More evidence is provided in Appendix B, where the variance of the packing fraction in both models is shown to match closely. There is building evidence that randomized topologies such as the CRG model, can approximate rigid spatial topologies when the local interactions in both topologies are matched. Apart from this paper, the strongest evidence to date for this line of reasoning is [43], where it was shown that the typical ensembles from the latent-space geometric graph model can be modeled by an inhomogeneous random graph model that matches with the original graph in terms of the average degree and a measure of clustering. We should mention that [43] is restricted to one-dimensional models and does not deal with sphere packing, but it shares with this paper the perspective that matching degrees and local clustering can be sufficient for describing spatial settings.

[1] J. Sanders, R. van Bijnen, E. Vredenbregt, and S. Kokkelmans, Phys. Rev. Lett. **112**, 163001 (2014).
[2] M. D. Lukin, M. Fleischhauer, R. Cote, L. M. Duan, D. Jaksch, J. I. Cirac, and P. Zoller, Phys. Rev. Lett. **87**, 37901 (2001).
[3] D. Jaksch, J. I. Cirac, P. Zoller, S. L. Rolston, R. Côté, and M. D. Lukin, Phys. Rev. Lett. **85**, 2208 (2000).
[4] M. Saffman, T. G. Walker, and K. Mølmer, Rev. Mod. Phys. **82**, 2313 (2010).
[5] J. Y. Chen, J. F. Klemic, and M. Elimelech, Nano Lett.

2, 393 (2002).
[6] L. M. Demers, D. S. Ginger, S. J. Park, Z. Li, S. W. Chung, and C. A. Mirkin, Science **296**, 1836 (2002).
[7] C. E. Shannon, SIGMOBILE Mob. Comput. Commun. Rev. **5**, 3 (2001).
[8] D. C. Gijswijt, H. D. Mittelmann, and A. Schrijver, IEEE Trans. Inf. Theory **58**, 2697 (2012).
[9] H. K. Kim and P. T. Toan, IEEE Trans. Inf. Theory **59**, 7337 (2013).
[10] H. Cohn and N. Elkies, Ann. Math. **157**, 689 (2003).
[11] H. Cohn, A. Kumar, S. D. Miller, D. Radchenko, and M. Viazovska, arXiv:1603.06518 (2016).
[12] T. C. Hales, Ann. Math. **162**, 1065 (2005).
[13] E. Hlawka, Mathematische Zeitschrift **49**, 285 (1943).
[14] M. Viazovska, arXiv:1603.04246 (2016).
[15] C. A. Rogers, Proc. London Math. Soc. **s3-8**, 609 (1958).
[16] S. Torquato, T. M. Truskett, and P. G. Debenedetti, Phys. Rev. Lett. **84**, 2064 (2000).
[17] S. Torquato and F. H. Stillinger, Exper. Math. **15**, 307 (2006).
[18] S. Torquato and F. H. Stillinger, Phys. Rev. E **73**, 031106 (2006).
[19] A. Cadilhe, N. A. M. Araújo, and V. Privman, J. Phys. Condens. Matter **19**, 65124 (2007).
[20] S. Torquato and F. H. Stillinger, Rev. Mod. Phys. **82**, 2633 (2010).
[21] S. Torquato, *Random heterogeneous materials: microstructure and macroscopic properties*, Vol. 16 (Springer-Verlag New York, 2013).
[22] M. D. Penrose and J. Yukich, Ann. Appl. Probab. **12**, 272 (2002).
[23] J. Dall and M. Christensen, Phys. Rev. E **66**, 016121 (2002).
[24] M. Barthélemy, Phys. Rep. **499**, 1 (2011).
[25] H. Solomon, in *Proc. Fifth Berkeley Symp. on Prob. and Stat*, Vol. 3 (1967) pp. 119–134.
[26] S. Torquato, O. U. Uche, and F. H. Stillinger, Phys. Rev. E **74**, 61308 (2006).
[27] G. Zhang and S. Torquato, Phys. Rev. E **88**, 53312 (2013).
[28] J. Talbot, P. Schaaf, and G. Tarjus, Mol. Phys. **72**, 1397 (1991).
[29] J. Feder, J. Theor. Biol. **87**, 237 (1980).
[30] F. Ball, T. Britton, and D. Sirl, J. Math. Biol. **66**, 979 (2013).
[31] E. Coupechoux and M. Lelarge, Adv. Appl. Probab. **46**, 985 (2014).
[32] P. Trapman, Theor. Popul. Biol. **71**, 160 (2007).
[33] M. E. J. Newman, Phys. Rev. Lett. **103**, 058701 (2009).
[34] B. Karrer and M. E. J. Newman, Phys. Rev. E **82**, 066118 (2010).
[35] C. Stegehuis, R. van der Hofstad, and J. S. H. van Leeuwaarden, Phys. Rev. E **94**, 012302 (2016).
[36] C. Stegehuis, R. van der Hofstad, and J. S. H. van Leeuwaarden, Sci. Rep. **6**, 29748 (2016).
[37] M. E. J. Newman, *Networks. An Introduction* (Oxford University Press, 2010).
[38] S. Dhara, J. S. H. van Leeuwaarden, and D. Mukherjee, J. Stat. Phys. **164**, 1217 (2016).
[39] G. Brightwell, S. Janson, and M. Luczak, arXiv:1510.05560 (2015).
[40] P. Bermolen, M. Jonckheere, and P. Moyal, arXiv:1310.8475 (2013).
[41] J. Sanders, M. Jonckheere, and S. Kokkelmans, Phys. Rev. Lett. **115** (2015).
[42] L. Devroye, A. György, G. Lugosi, and F. Udina, Electron. J. Probab. **16**, 2481 (2011).
[43] D. Krioukov, Phys. Rev. Lett. **116**, 208302 (2016), 1604.01575.
[44] P. Bermolen, M. Jonckheere, and J. Sanders, arXiv:1504.02438 (2015), arXiv:1504.02438.
[45] I. Karatzas and S. E. Shreve, *Brownian Motion and Stochastic Calculus*, Vol. 113 (Springer-Verlag, New York, 1991) p. 470.
[46] R. Liptser and A. Shiryaev, *Theory of Martingales* (Springer, 1989).
[47] S. N. Ethier and T. G. Kurtz, *Markov Processes: Characterization and Convergence* (John Wiley & Sons, 2009).
[48] G. Pang, R. Talreja, and W. Whitt, Probability Surveys **4**, 193 (2007), arXiv:0712.4211.
[49] W. Whitt, *Stochastic-Process Limits*, Springer Series in Operations Research and Financial Engineering (Springer-Verlag, New York, 2002).
[50] L. Arnold, *Stochastic Differential Equations: Theory and Applications* (John Wiley & Sons, 1974).
[51] S. Li, Asian Journal of Mathematics & Statistics **4**, 66 (2011).

Appendix A: Asymptotic analysis of the CRG model

Here we analyze the asymptotic properties of RSA on the $\mathrm{CRG}(c,\alpha)$ model. We introduce an algorithm that sequentially activates the vertices while obeying the hard-core exclusion constraint, and then analyze the exploration algorithm (see [38, 39, 44] for similar analyses in various other contexts). For each vertex, the neighbors inside and outside its own household will be referred to as 'household neighbors' and 'distant neighbors', respectively. If H denotes the number of household neighbors of a typical vertex, then observe that $H \sim \mathrm{Poisson}(\alpha c)$. Therefore, $\mathbb{E}(H) = \alpha c$, and $\mathrm{Var}(H) = \alpha c$. Furthermore, any two vertices belonging to two different households are connected by an edge with probability $p_n = (1-\alpha)c/n$, so the number of distant neighbors is a $\mathrm{Bin}(n-H-1, p_n)$ random variable, $\mathrm{Poisson}((1-\alpha)c)$ in the large n limit. Notice that the total number of neighbors, is then asymptotically given by a $\mathrm{Poisson}(c)$ random variable. For a $\mathrm{CRG}(c,\alpha)$ model on n vertices, denote the fraction of active vertices after the RSA process reached a jammed state by $\hat{J}_n(c,\alpha)$. In this section we fix $c > 0$ and $\alpha \in [0,1]$, and simply write $\hat{J}_n$ for $\hat{J}_n(c,\alpha)$.

Notation. Write $\mu = 1 + \alpha c$, $\lambda = (1-\alpha)c$, and $\sigma^2 = \alpha c$. Note that μ denotes the expected size of the household containing a typical vertex, since a household contains a vertex and its household neighbors. In the proof, we use boldfaced letters to denote stochastic processes, and vectors. Terms like 'vertex' or 'node' will be used interchangeably.

A sequence of random variables $\{X_n\}_{n\geq 1}$ is said to be $O_{\mathbb{P}}(f(n))$, or $o_{\mathbb{P}}(f(n))$, for some function $f:\mathbb{R}\to\mathbb{R}_+$, if the sequence of scaled random variables $\{X_n/f(n)\}_{n\geq 1}$ is tight, or converges to zero in probability, respectively. We denote by $D_E[0,\infty)$ the set of all *cádlág* (right continuous left limit exists) functions from $[0,\infty)$ to a complete, separable metric space E, endowed with the Skorohod J_1 topology, and by '$\xrightarrow{d}$' and '$\xrightarrow{\mathbb{P}}$', convergence in distribution and in probability, respectively. In particular, if the sample paths of a stochastic process $\mathbf{X}$ are continuous, we write $\mathbf{X}_n = \{X_n(t)\}_{t\geq 0} \xrightarrow{d} \mathbf{X} = \{X(t)\}_{t\geq 0}$, if for any $T \geq 0$,

$$\sup_{t\in[0,T]} |X_n(t) - X(t)| \xrightarrow{\mathbb{P}} 0 \quad \text{as} \quad n\to\infty. \tag{A1}$$

1. Main result

The following result proves the central limit theorem (CLT) for $\hat{J}_n$.

Theorem 2 (CLT for jamming fraction)**.** *As $n\to\infty$,*

$$\sqrt{n}(\hat{J}_n - \hat{J}) \xrightarrow{d} \mathcal{N}(0,\hat{V}),$$

where $\hat{J}$ is the smallest non-negative root of the deterministic function

$$x(t) = e^{-\lambda t}(1-\mu t)^{\frac{\mu-1}{\mu}}\left(1 - \int_0^t e^{\lambda s}(1-\mu s)^{-1+\frac{1}{\mu}}\mathrm{d}s\right), \quad t < \frac{1}{\mu}, \tag{A2}$$

and $\hat{V} = \sigma_{xx}(\hat{J})$ with $\sigma_{xx}(t)$ the unique solution of the system of differential equations

$$\begin{aligned} \frac{\mathrm{d}\sigma_{xx}(t)}{\mathrm{d}t} &= 2\sigma_{xx}(t)f(t) + 2\sigma_{xy}(t)g(t) + \beta(t), \\ \frac{\mathrm{d}\sigma_{xy}(t)}{\mathrm{d}t} &= \sigma_{xy}(t)f(t) + tg(t)\sigma^2 + \sqrt{\beta(t)}\sigma\rho(t) \end{aligned} \tag{A3}$$

for $0\leq t < 1/\mu$, with

$$\begin{aligned} &y(t) = 1-\mu t,\ f(t) = -\frac{\mu-1}{y(t)} - \lambda,\ g(t) = \frac{(\mu-1)x(t)}{y(t)^2}, \\ &\beta(t) = \left[\frac{(\mu-1)}{y(t)} + \lambda\right]x(t),\ \rho(t) = \frac{\sigma}{\sqrt{\beta(t)}}\frac{x(t)}{y(t)}. \end{aligned} \tag{A4}$$

Theorem 2 says that for large n, the fraction of active vertices in the jammed state will be approximately given by $(\hat{J}\cdot n + Z\cdot\sqrt{n})$, where Z is a Normal random variable with mean 0 and variance $\hat{V}$. The next theorem establishes that for large c, $\hat{J}(c,\alpha)\sim(1+c\alpha)^{-1}$, which is a simple law for the jamming fraction in the high-density regime.

Theorem 3 (Large density regime)**.** *As $c\to\infty$, $(1+c\alpha)\hat{J}(c,\alpha)\to 1$.*

2. The exploration algorithm

Instead of fixing a particular realization of the random graph and then studying RSA on that given graph, we will sequentially *activate* the vertices one-by-one, *explore* the neighborhood of the activated vertices, and construct the random topology of the graph. The idea of exploring this way simplifies the whole analysis, since the evolution of the system can be described recursively in terms of the previous states. Similar constructions have been displayed for other random graph models in the literature [38, 41]. Below we describe the specific algorithm for the CRG model.

Observe that during the process of sequential activation, until the jamming state is reached, the vertices can be in either of three states: active, blocked, and unexplored (i.e. vertices with future potential activation). Furthermore, there can be two types of blocked vertices: (i) blocked due to activation of some household neighbor, or (ii) none of the household neighbors is active, but there is an active distant neighbor. Therefore, at each time $t\geq 0$, categorize the vertices into four sets:

- $\mathrm{A}(t)$: set of all vertices active.
- $\mathrm{U}(t)$: set of all vertices that are not active and that have not been blocked by any vertex in $\mathrm{A}(t)$.
- $\mathrm{BH}(t)$: set of all vertices that belong to a household of some vertex in $\mathrm{A}(t)$.
- $\mathrm{BO}(t)$: set of all vertices that do not belong to a household yet, but are blocked due to connections with some vertex in $\mathrm{A}(t)$ as a distant neighbor.

Note that $\mathrm{BH}(t) \cup \mathrm{BO}(t)$ constitute the set of all blocked vertices at time t, and $\mathrm{BH}(t) \cap \mathrm{BO}(t) = \emptyset$. Initially, all vertices are unexplored, so that $\mathrm{U}(0) = V(G)$, the set of all n vertices. At time step t, one vertex v is selected from $\mathrm{U}(t-1)$ uniformly at random and is transferred to $\mathrm{A}(t)$, i.e., one unexplored vertex becomes active.

We now explore the neighbors of v, which can be of two types: the household neighbors, and the distant neighbors. Further observe that v can have its household neighbors only from the set $\mathrm{U}(t-1) \cup \mathrm{BO}(t-1) \setminus \{v\}$, since each vertex in $\mathrm{BH}(t-1)$ already belongs to some household. Define

$$H(t) \sim \min\Big\{\mathrm{Poisson}(\alpha c), |\mathrm{U}(t-1) \cup \mathrm{BO}(t-1) \setminus \{v\}|\Big\},$$

i.e., draw a $\mathrm{Poisson}(\alpha c)$ random variable independently of any other process, and if it is smaller than $|\mathrm{U}(t-1) \cup \mathrm{BO}(t-1) \setminus \{v\}|$, then take it to be the value of H, and otherwise set $H(t) = |\mathrm{U}(t-1) \cup \mathrm{BO}(t-1) \setminus \{v\}|$. Select $H(t)$ vertices $\{u_1, u_2, \ldots, u_H\}$ at random from all vertices in $U(t-1) \cup \mathrm{BO}(t-1) \setminus \{v\}$. These $H(t)$ vertices together form the household containing v, and are moved to $\mathrm{BH}(t)$, irrespective of the set they are selected from. To explore the distant neighbors, select one by one, all the vertices in $\mathrm{U}(t-1) \cup \mathrm{BO}(t-1) \cup \mathrm{BH}(t-1) \setminus \{v, u_1, \ldots, u_H\}$, and for every such selected vertex $\bar{u}$, put an edge between $\bar{u}$ and v with probability p_n. Denote the newly created distant neighbors that belonged to $\mathrm{U}(t-1)$ by $\{\bar{u}_1, \ldots, \bar{u}_d\}$, and move these vertices to $\mathrm{BO}(t)$. In summary, the exploration algorithm yields the following recursion relations:

$$\begin{aligned}
\mathrm{A}(t) &= \mathrm{A}(t-1) \cup \{v\},\\
\mathrm{U}(t) &= \mathrm{U}(t-1) \setminus \{v, u_1, u_2, \ldots, u_H, \bar{u}_1, \ldots, \bar{u}_d\},\\
\mathrm{BH}(t) &= \mathrm{BH}(t-1) \cup \{u_1, u_2, \ldots, u_H\},\\
\mathrm{BO}(t) &= \mathrm{BO}(t-1) \cup \{\bar{u}_1, \ldots, \bar{u}_d\}.
\end{aligned}$$

The algorithm terminates when there is no vertex left in the set $\mathrm{U}(t)$ (implying that all vertices are either active or blocked), and outputs the cardinality of $\mathrm{A}(t)$ as the number of active vertices in the jammed state.

3. State description and martingale decomposition.

Denote for $t \geq 0$,

$$X_n(t) := |\mathrm{U}(t)|, \quad Y_n(t) := |\mathrm{U}(t) \cup \mathrm{BO}(t)|.$$

Observe that $\{(X_n(t), Y_n(t))\}_{t \geq 0}$ is a Markov chain. At each time step, one new vertex becomes active, so that $|\mathrm{A}(t)| = t$, and the total number of vertices in the jammed state is given by the time step when $X_n(t)$ hits zero, i.e., the time step when the exploration algorithm terminates.

Dynamics of X_n. First we make the following observations:

- $X_n(t)$ decreases by one, when a new vertex v becomes active.
- The household neighbors of v are selected from $Y_n(t-1)$ vertices, and $X_n(t)$ decreases by an amount of the number of such vertices which are in $\mathrm{U}(t-1)$.
- $X_n(t)$ decreases by the number of distant neighbors of the newly active vertex that belong to $\mathrm{U}(t-1)$ (since they are transferred to $\mathrm{BO}(t)$).

Thus,

$$X_n(t+1) = X_n(t) - \xi_n(t+1) \quad \text{and} \quad X_n(0) = n \tag{A5}$$

with

$$\xi_n(t+1) = 1 + \eta_1(t+1) + \eta_2(t+1), \tag{A6}$$

where conditionally on $(X_n(t), Y_n(t))$,

$$\eta_1(t+1) \sim \text{Hypergeometric}(X_n(t), Y_n(t), H(t)), \tag{A7}$$

i.e., $\eta_1(t+1)$ has a Hypergeometric distribution with favorable outcomes $X_n(t)$, population size $Y_n(t)$, and sample size $H(t)$. Further, conditionally on $(X_n(t), Y_n(t), \eta_1(t+1))$,

$$\eta_2(t+1) \sim \text{Bin}\Big(X_n(t) - 1 - \eta_1(t+1),\ \frac{\lambda}{n}\Big). \tag{A8}$$

Therefore, the drift function of the $\mathbf{X}_n$ process satisfies

$$\begin{aligned}\mathbb{E}\left(\xi_n(t+1)|X_n(t), Y_n(t)\right) &= 1 + \frac{X_n(t)(\mu-1)}{Y_n(t)} + \left(X_n(t) - 1 - \frac{X_n(t)(\mu-1)}{Y_n(t)}\right)\frac{\lambda}{n} \\ &= 1 + \frac{X_n(t)(\mu-1)}{Y_n(t)} + \frac{\lambda X_n(t)}{n} + O_{\mathbb{P}}(n^{-1}),\end{aligned} \tag{A9}$$

where, in the last step, we have used the fact that $X_n(t) \le Y_n(t)$.

Dynamics of Y_n. The value of Y_n does not change due to the creation of distant neighbors. At time t, it can only decrease due to an activation of a vertex v (since it is moved to $\mathrm{A}(t)$), and the formation of a household, since all the vertices that make the household of v, were in $\mathrm{U}(t-1) \cup \mathrm{BO}(t-1)$, and are moved to $\mathrm{BH}(t)$. Thus, at each time step, $Y_n(t)$ decreases on average by an amount $\mu = 1 + \alpha c$, the expected household size, except at the final step when the residual number of vertices can be smaller than the household size. But this will not affect our asymptotic results in any way, and we will ignore it. Hence,

$$Y_n(t+1) = Y_n(t) - \zeta_n(t+1) \quad \text{and} \quad Y_n(0) = n, \tag{A10}$$

where

$$\mathbb{E}\left(\zeta_n(t+1)|X_n(t), Y_n(t)\right) = \mu. \tag{A11}$$

Martingale decomposition. Using the Doob-Meyer decomposition [45, Theorem 4.10] of $\boldsymbol{X}_n$, (A9) yields the following martingale decomposition

$$X_n(t) = n - \sum_{i=1}^{t} \xi_n(i) = n + M_n^X(t) - t - \sum_{i=1}^{t}\left[\frac{X_n(i-1)(\mu-1)}{Y_n(i-1)} + \frac{\lambda X_n(i-1)}{n} + O_{\mathbb{P}}(n^{-1})\right],$$

where $\boldsymbol{M}_n^X = \{M_n^X(t)\}_{t\ge1}$ is a square-integrable martingale with respect to a suitable filtration. Let us now define the scaled processes

$$x_n(t) := \frac{X_n(\lfloor nt \rfloor)}{n} \quad \text{and} \quad y_n(t) := \frac{Y_n(\lfloor nt \rfloor)}{n}.$$

Also define

$$\delta(x, y) := (\mu - 1)\frac{x}{y} + \lambda x, \quad \text{for} \quad 0 \le x \le y,\ y > 0. \tag{A12}$$

Thus, we can write

$$\begin{aligned}x_n(t) &= 1 + \frac{M_n^X(\lfloor nt \rfloor)}{n} - \frac{\lfloor nt \rfloor}{n} - \frac{1}{n}\sum_{i=1}^{\lfloor nt \rfloor}\delta\Big(\frac{X_n(i-1)}{n}, \frac{Y_n(i-1)}{n}\Big) + O_{\mathbb{P}}(n^{-1}) \\ &= 1 + \frac{M_n^X(\lfloor nt \rfloor)}{n} - t - \int_0^t \delta(x_n(s), y_n(s))\mathrm{d}s + O_{\mathbb{P}}(n^{-1}).\end{aligned} \tag{A13}$$

Similar arguments yield

$$y_n(t) = 1 + \frac{M_n^Y(\lfloor nt \rfloor)}{n} - \mu t + O_{\mathbb{P}}(n^{-1}), \tag{A14}$$

where $\boldsymbol{M}_n^Y = \{M_n^Y(t)\}_{t\ge1}$ is a square-integrable martingale with respect to a suitable filtration. We write $\boldsymbol{x}_n$ and $\boldsymbol{y}_n$ to denote the processes $(x_n(t))_{t\ge0}$ an $(y_n(t))_{t\ge0}$ respectively.

4. Proof outline

The proof of Theorem 2 consists of three key steps: First we show that the processes $\boldsymbol{x}_n$ and $\boldsymbol{y}_n$ converges in probability to deterministic functions. This shows that the fraction $\hat{J}_n$ converge in probability to some deterministic limit $\hat{J}$. Next, in Proposition 7, we show that the diffusion-scaled processes (defined in (A41)) converges to a two-dimensional Ornstein-Uhlenbeck process. Finally, the scaled fluctuations around $\hat{J}$ of $\hat{J}_n$ are shown to have a Gaussian limit, as stated in Theorem 2.

5. Quadratic variation and covariation

To investigate the scaling behavior of the martingales, we will now compute the quadratic variation and covariation terms. For convenience, denote by $\mathbb{P}_t, \mathbb{E}_t$, Var_t, Cov_t, the conditional probability, expectation, variance and covariance, respectively, conditioned on $(X_n(t), Y_n(t))$. Notice that, for the martingales $\boldsymbol{M}_n^X$ and $\boldsymbol{M}_n^Y$, the quadratic variation and covariation terms are given by

$$\begin{aligned}
\langle M_n^X\rangle(\lfloor nt\rfloor) &= \sum_{i=1}^{\lfloor nt\rfloor} \mathrm{Var}_{i-1}(\xi_n(i)),\\
\langle M_n^Y\rangle(\lfloor nt\rfloor) &= \sum_{i=1}^{\lfloor nt\rfloor} \mathrm{Var}_{i-1}(\zeta_n(i)),\\
\langle M_n^X, M_n^Y\rangle(\lfloor nt\rfloor) &= \sum_{i=1}^{\lfloor nt\rfloor} \mathrm{Cov}_{i-1}(\zeta_n(i), \xi_n(i)).
\end{aligned} \tag{A15}$$

Thus, the quantities of interest are $\mathrm{Var}_t(\xi_n(t+1))$, $\mathrm{Var}_t(\zeta_n(t+1))$ and $\mathrm{Cov}_t(\xi_n(t+1), \zeta_n(t+1))$, which we derive in the three successive claims.

Claim 1. *For any $t \geq 1$,*

$$\mathrm{Var}_t(\zeta_n(t+1)) = \sigma^2. \tag{A16}$$

Proof. The proof is immediate by observing that the random variable denoting the household size has variance σ^2. □

Claim 2. *For any $t \geq 1$,*

$$\mathrm{Var}_t\left(\xi_n(t+1)\right) = \frac{X_n(t)(\mu-1)}{Y_n(t)} + \frac{\lambda X_n(t)}{n} + O_{\mathbb{P}}(n^{-1}). \tag{A17}$$

Proof. From the definition of ξ_n in (A6), the computation of $\mathrm{Var}_t(\xi_n(t+1))$ requires computation of $\mathrm{Var}_t(\eta_1(t+1))$, $\mathrm{Cov}_t(\eta_1(t+1), \eta_2(t+1))$ and $\mathrm{Var}_t(\eta_2(t+1))$. Since η_1 follows a Hypergeometric distribution,

$$\mathbb{E}_t\left(\eta_1(t+1)(\eta_1(t+1)-1)|H\right) = \frac{X_n(t)(X_n(t)-1)(H-1)(H-2)}{Y_n(t)(Y_n(t)-1)} \tag{A18}$$

and

$$\begin{aligned}
\mathrm{Var}_t\left(\eta_1(t+1)\right) &= \frac{X_n(t)(X_n(t)-1)\mathbb{E}\left((H-1)(H-2)\right)}{Y_n(t)(Y_n(t)-1)} + \mathbb{E}_t\left(\eta_1(t+1)\right) - \mathbb{E}_t^2\left(\eta_1(t+1)\right)\\
&= \frac{X_n^2(t)}{Y_n^2(t)}(\sigma^2+\mu^2-3\mu+2) + \frac{X_n(t)}{Y_n(t)}(\mu-1) - \frac{X_n^2(t)}{Y_n^2(t)}(\mu-1)^2 + O_{\mathbb{P}}(n^{-1})\\
&= \frac{X_n^2(t)}{Y_n^2(t)}(\sigma^2-\mu+1) + \frac{X_n(t)}{Y_n(t)}(\mu-1) + O_{\mathbb{P}}(n^{-1})\\
&= \frac{X_n(t)}{Y_n(t)}(\mu-1) + O_{\mathbb{P}}(n^{-1}),
\end{aligned} \tag{A19}$$

since $\sigma^2 = \mu - 1 = \alpha c$. Also, we have

$$\begin{aligned}
&\mathbb{E}_t\left(\eta_2(t+1)(\eta_2(t+1)-1)\right) \\
&= \left[(X_n(t)-1)(X_n(t)-2) - \mathbb{E}_t\left(\eta_1(t+1)\right)\left[2X_n(t)-3\right] + \mathbb{E}_t\left(\eta_1^2(t+1)\right)\right]\left(\frac{\lambda}{n}\right)^2 \\
&= \frac{\lambda^2 X_n^2(t)}{n^2} + O_{\mathbb{P}}(n^{-1})
\end{aligned} \tag{A20}$$

and therefore

$$\mathrm{Var}_t(\eta_2(t+1)) = \frac{\lambda X_n(t)}{n} + O_{\mathbb{P}}(n^{-1}). \tag{A21}$$

Further,

$$\begin{aligned}
\mathbb{E}_t\left(\eta_1(t+1)\eta_2(t+1)\right) &= \mathbb{E}_t\left(\eta_1(t+1)(X_n(t)-1-\eta_1(t+1))\frac{\lambda}{n}\right) \\
&= \frac{\lambda}{n}\left[(X_n(t)-1)\mathbb{E}_t(\eta_1(t+1)) - \mathbb{E}_t(\eta_1^2(t+1))\right] \\
&= \frac{\lambda X_n(t)}{n}\frac{X_n(t)(\mu-1)}{Y_n(t)} + O_{\mathbb{P}}(n^{-1}).
\end{aligned} \tag{A22}$$

Now, from (A7), (A8),

$$\mathbb{E}_t(\eta_1(t+1)) = \frac{\lambda X_n(t)}{n} + O_{\mathbb{P}}(n^{-1}) \quad \text{and} \quad \mathbb{E}_t(\eta_2(t+1)) = \frac{X_n(t)(\mu-1)}{Y_n(t)} + O_{\mathbb{P}}(n^{-1}),$$

which implies that

$$\mathrm{Cov}_t(\eta_1(t+1), \eta_2(t+1)) = O_{\mathbb{P}}(n^{-1}). \tag{A23}$$

Combining (A19), (A21) and (A23), gives (A17). □

Claim 3. *For any $t \geq 1$,*

$$\mathrm{Cov}_t\left(\zeta_n(t+1), \xi_n(t+1)\right) = \frac{X_n(t)}{Y_n(t)}\sigma^2 + O_{\mathbb{P}}(n^{-1}). \tag{A24}$$

Proof. First, observe that

$$\begin{aligned}
&\mathbb{E}_t\left(\zeta_n(t+1)\eta_1(t+1)\right) = \mathbb{E}_t\left(\zeta_n(t+1)\mathbb{E}_t\left(\eta_1(t+1)|\zeta_n(t+1)\right)\right) \\
&= \frac{X_n(t)}{Y_n(t)}\mathbb{E}_t\left(\zeta_n(t+1)(\zeta_n(t+1)-1)\right) = \frac{X_n(t)}{Y_n(t)}(\sigma^2+\mu^2-\mu),
\end{aligned} \tag{A25}$$

and therefore,

$$\mathrm{Cov}_t(\zeta_n(t+1), \eta_1(t+1)) = \frac{X_n(t)}{Y_n(t)}\sigma^2. \tag{A26}$$

Thus,

$$\begin{aligned}
&\mathbb{E}_t\left(\zeta_n(t+1)\eta_2(t+1)\right) = \mathbb{E}_t\left(\zeta_n(t+1)\mathbb{E}_t\left(\eta_2(t+1)|\eta_1(t+1), \zeta_n(t+1)\right)\right) \\
&= \mathbb{E}_t\left(\zeta_n(t+1)(X_n(t)-1-\eta_1(t+1))\frac{\lambda}{n}\right) = \lambda\mu\frac{X_n(t)}{n} + O_{\mathbb{P}}(n^{-1})
\end{aligned} \tag{A27}$$

and hence

$$\mathrm{Cov}_t\left(\zeta_n(t+1), \eta_2(t+1)\right) = O_{\mathbb{P}}(n^{-1}). \tag{A28}$$

Combining (A26) and (A28) yields (A24). □

6. Convergence of the exploration process on n-scale

Based on the quadratic variation and covariation results in Section A 5, the following lemma shows that the martingales when scaled by n, converge to the zero-process.

Lemma 4. *For any fixed $T \geq 0$, as $n \to \infty$,*

$$\frac{1}{n}\sup_{t\leq T}|\boldsymbol{M}_n^X(\lfloor nt\rfloor)| \xrightarrow{\mathbb{P}} 0, \quad \frac{1}{n}\sup_{t\leq T}|\boldsymbol{M}_n^Y(\lfloor nt\rfloor)| \xrightarrow{\mathbb{P}} 0. \tag{A29}$$

Proof. Observe that using (A15) along with (A16) and (A17), we can claim for any $T \geq 0$,

$$\langle \boldsymbol{M}_n^X\rangle(\lfloor nT\rfloor) = O_{\mathbb{P}}(n), \quad \langle \boldsymbol{M}_n^Y\rangle(\lfloor nT\rfloor) = O_{\mathbb{P}}(n). \tag{A30}$$

Thus, from Doob's inequality [46, Theorem 1.9.1.3], the proof follows. □

Proposition 5 (Functional LLN of the exploration process)**.** *As $n \to \infty$, the processes $\{x_n(t)\}_{0\leq t<1/\mu}$ and $\{y_n(t)\}_{0\leq t<1/\mu}$ converge weakly to the deterministic processes $\{x(t)\}_{0\leq t<1/\mu}$ and $\{y(t)\}_{0\leq t<1/\mu}$, respectively, where $y(t) = 1-\mu t$ and $x(t)$ is the unique, non-increasing, continuous function satisfying*

$$x(t) = 1 - t - \int_0^t \left(\frac{\mu - 1}{1-\mu s} + \lambda\right) x(s)\mathrm{d}s, \quad 0 \leq t < 1/\mu. \tag{A31}$$

Proof. Recall the representations of $\boldsymbol{x}_n$, and $\boldsymbol{y}_n$ from (A13) and (A14). Fix any $0 \leq T < 1/\mu$. Observe that Lemma 4 immediately yields

$$\sup_{t\leq T}|y_n(t) - y(t)| \xrightarrow{\mathbb{P}} 0. \tag{A32}$$

Next note that $\delta(x, y)$, as defined in (A12), is Lipschitz continuous on $[0, 1] \times [\epsilon, 1]$ for any $\epsilon > 0$ and we can choose this $\epsilon > 0$ in such a way that $y(t) \geq \epsilon$ for all $t \leq T$ (since $T < 1/\mu$). Therefore, the Lipschitz continuity of δ implies that there exists a constant $C > 0$ such that

$$\sup_{t\leq T}|\delta(x_n(t), y_n(t)) - \delta(x(t), y(t))| \leq C\Big(\sup_{t\leq T}|x_n(t) - x(t)| + \sup_{t\leq T}|y_n(t) - y(t)|\Big). \tag{A33}$$

Thus,

$$\begin{aligned}
\sup_{t\leq T}|x_n(t) - x(t)| &\leq \sup_{t\leq T}\frac{|M_n^X(\lfloor nt\rfloor)|}{n} + \int_0^T \sup_{t\leq u}|\delta(x_n(t), y_n(t)) - \delta(x(t), y(t))|\mathrm{d}u + o_{\mathbb{P}}(1)\\
&\leq \sup_{t\leq T}\frac{|M_n^X(\lfloor nt\rfloor)|}{n} + C\int_0^T \sup_{t\leq u}|x_n(u) - x(u)|\mathrm{d}u + C\int_0^T \sup_{t\leq u}|y_n(u) - y(u)|\mathrm{d}u + o_{\mathbb{P}}(1)\\
&\leq \varepsilon_n + C\int_0^T \sup_{t\leq u}|x_n(t) - x(t)|\mathrm{d}u,
\end{aligned}$$

where, by Lemma 4 and (A32),

$$\varepsilon_n := \sup_{t\leq T}\frac{|M_n^X(\lfloor nt\rfloor)|}{n} + CT\sup_{t\leq T}|y_n(t) - y(t)| + o_{\mathbb{P}}(1),$$

which converges in probability to zero, as $n \to \infty$. Using Grőnwall's inequality [47, Theorem 5.1], we get

$$\sup_{t\leq T}|x_n(t) - x(t)| \leq \varepsilon_n e^{CT} \xrightarrow{\mathbb{P}} 0, \tag{A34}$$

and the proof is now complete. □

7. Properties of the limiting function

In this subsection, we characterize $\boldsymbol{x}$ explicitly, and derive some of its properties. Notice that the integral recursion equation (A31) can be expressed as a linear differential equation with $x(0) = 1$, and

$$\begin{aligned} & x'(t) = -1 - \left(\frac{\mu-1}{1-\mu t} + \lambda\right) x(t) \\ \implies \quad & x'(t) + \left(\frac{\mu-1}{1-\mu t} + \lambda\right) x(t) = -1 \\ \implies \quad & r(t)x'(t) + r(t)\left(\frac{\mu-1}{1-\mu t} + \lambda\right) x(t) = -r(t), \end{aligned} \tag{A35}$$

where the function $r(t)$ is such that $r(0) = 1$ and

$$\begin{aligned} & r'(t) = r(t)\left(\frac{\mu-1}{1-\mu t} + \lambda\right) \\ \implies \quad & \frac{r'(t)}{r(t)} = \frac{\mu-1}{1-\mu t} + \lambda \\ \implies \quad & \log(r(t)) = -\frac{\mu-1}{\mu}\log(1-\mu t) + \lambda t + C \\ \implies \quad & r(t) = (1-\mu t)^{-\frac{\mu-1}{\mu}} e^{\lambda t}. \quad C = 0, \text{ as } r(0) = 1. \end{aligned} \tag{A36}$$

Thus, (A35) now implies

$$\begin{aligned} & r(t)x(t) - r(0)x(0) = -\int_0^t r(s)\mathrm{d}s \\ \implies \quad & x(t) = e^{-\lambda t}(1-\mu t)^{\frac{\mu-1}{\mu}}\left(1 - \int_0^t e^{\lambda s}(1-\mu s)^{-1+\frac{1}{\mu}}\mathrm{d}s\right), \quad t < \frac{1}{\mu}. \end{aligned} \tag{A37}$$

The smallest root of the integral equation (A31) defined a $\hat{J}$, must be the smallest positive solution of

$$\int_0^t e^{\lambda s}(1-\mu s)^{-1+\frac{1}{\mu}}\mathrm{d}s = 1. \tag{A38}$$

The claim below establishes that such a $\hat{J} < 1/\mu$ exists.

Claim 4. *Let $\hat{J} := \inf\{t : x(t) = 0\}$, where $\boldsymbol{x}$ is given by* (A2)*. Then $\hat{J} < 1/\mu$.*

Proof. The integrand in the left hand side of (A38) is positive, and tends to ∞ as t increases to $1/\mu$. Therefore, the integral $\int_0^t e^{\lambda s}(1-\mu s)^{-1+1/\mu}\mathrm{d}s$ tends to infinity as well. Thus, there must exist a solution of (A38) which is smaller that $1/\mu$, and the proof follows. □

Next we prove Theorem 3, which shows that although for fixed μ, $\hat{J} < 1/\mu$, as μ grows large, $\hat{J}$ becomes arbitrarily close to $1/\mu$.

Proof of Theorem 3. Note that in the current notation an equivalent restatement is that as $\mu \to \infty$, $\mu\hat{J} \to 1$. In this proof $\hat{J}$ should be understood as a function of μ and λ. Observe that, for $t < 1/\mu$,

$$\begin{aligned} & 1 - \int_0^t e^{\lambda s}(1-\mu s)^{-1+\frac{1}{\mu}}\mathrm{d}s \geq 1 - e^{\lambda t}(1-\mu t)^{\frac{1}{\mu}}\int_0^t (1-\mu s)^{-1}\mathrm{d}s \\ & \geq 1 - e^{\lambda t}(1-\mu t)^{\frac{1}{\mu}}\left[-\frac{1}{\mu}\log(1-\mu s)\right]_0^t \sim 1 - e^{\frac{\lambda}{\mu}}\frac{1}{\mu}\log(1-\mu t), \end{aligned} \tag{A39}$$

and

$$1 - e^{\frac{\lambda}{\mu}}\frac{1}{\mu}\log(1-\mu t) = 0, \implies t = \frac{1}{\mu}(1 - e^{-\mu e^{-\frac{\lambda}{\mu}}}) \sim \frac{1}{\mu} \text{ as } \mu \to \infty. \tag{A40}$$

Since $\hat{J} \geq (1 - e^{-\mu e^{-\frac{\lambda}{\mu}}})$, the proof follows. □

8. Convergence of exploration process on diffusion scale

Define the diffusion-scaled processes

$$\bar{X}_n(t) := \sqrt{n}(x_n(t) - x(t)), \quad \bar{Y}_n(t) := \sqrt{n}(y_n(t) - y(t)), \tag{A41}$$

and the diffusion-scaled martingales

$$\bar{M}_n^X(t) := \frac{M_n^X(\lfloor nt \rfloor)}{\sqrt{n}}, \quad \bar{M}_n^Y(t) := \frac{M_n^Y(\lfloor nt \rfloor)}{\sqrt{n}}.$$

Now observe from (A13) that

$$\begin{aligned}\bar{X}_n(t) &= \bar{M}_n^X(t) - (\mu-1)\left[\int_0^t \frac{\bar{X}_n(s)}{y_n(s)}\mathrm{d}s + \int_0^t x(s)\sqrt{n}\left(\frac{1}{y_n(s)} - \frac{1}{y(s)}\right)\mathrm{d}s\right] - \lambda\int_0^t \bar{X}_n(s)\mathrm{d}s + O_{\mathbb{P}}(n^{-1/2}) \\ &= \bar{M}_n^X(t) - (\mu-1)\int_0^t \frac{\bar{X}_n(s)}{y_n(s)}\mathrm{d}s + \int_o^t \frac{x(s)(\mu-1)}{y_n(s)y(s)}\bar{Y}_n(s)\mathrm{d}s - \lambda\int_0^t \bar{X}_n(s)\mathrm{d}s + o_{\mathbb{P}}(1).\end{aligned}$$

Therefore, we can write

$$\bar{X}_n(t) = \bar{M}_n^X(t) + \int_0^t f_n(s)\bar{X}_n(s)\mathrm{d}s + \int_0^t g_n(s)\bar{Y}_n(s)\mathrm{d}s + o_{\mathbb{P}}(1), \tag{A42}$$

where

$$f_n(t) = -\frac{(\mu-1)}{y_n(t)} - \lambda, \qquad g_n(t) = \frac{(\mu-1)x(t)}{y_n(t)y(t)}. \tag{A43}$$

Furthermore, (A14) yields

$$\bar{Y}_n(t) = \sqrt{n}(y_n(t) - y(t)) = \bar{M}_n^Y(t) + o_{\mathbb{P}}(1), \tag{A44}$$

Based on the quadratic variation and covariation results in Section A 5, the following lemma shows that the martingales when scaled by $\sqrt{n}$ converge to a diffusion process described by an SDE.

Lemma 6 (Diffusion limit of martingales)**.** *As $n \to \infty$, $(\bar{\boldsymbol{M}}_n^X, \bar{\boldsymbol{M}}_n^Y) \xrightarrow{d} (\boldsymbol{W}_1, \boldsymbol{W}_2)$, where the process $(\boldsymbol{W}_1, \boldsymbol{W}_2)$ is described by the* SDE

$$\mathrm{d}W_1(t) = \sqrt{\beta(t)}\left[\rho(t)\mathrm{d}B_1(t) + \sqrt{1-\rho(t)^2}\mathrm{d}B_2(t)\right], \quad \mathrm{d}W_2(t) = \sigma\mathrm{d}B_1(t), \tag{A45}$$

where $\boldsymbol{B}_1$ and $\boldsymbol{B}_2$ are two independent standard Brownian motions.

Proof. The idea is to use the martingale functional central limit theorem (cf. [48, Theorem 8.1]), where the convergence of the martingales are characterized by the convergence of their quadratic variation process. Using the functional LLN obtained in Proposition 5, we compute the asymptotics of the quadratic variations and covariation of $\bar{\boldsymbol{M}}_n^X$ and $\bar{\boldsymbol{M}}_n^Y$. From (A13) and (A16), we obtain

$$\langle \bar{M}_n^Y \rangle(t) = \frac{1}{n}\sum_{i=1}^{\lfloor nt \rfloor} \mathrm{Var}_{i-1}(\zeta_n(i)) \xrightarrow{\mathbb{P}} \sigma^2 t.$$

Again, (A13), (A17) and Proposition 5 yields

$$\langle \bar{M}_n^X \rangle(t) = \frac{1}{n}\sum_{i=1}^{\lfloor nt \rfloor} \mathrm{Var}_{i-1}(\xi_n(i)) \xrightarrow{\mathbb{P}} \int_0^t \left[\frac{(\mu-1)}{y(s)} + \lambda\right] x(s)\mathrm{d}s = \int_0^t \beta(s)\mathrm{d}s.$$

Finally, from (A13), (A24) and Proposition 5 we obtain

$$\langle \bar{M}_n^X, \bar{M}_n^Y \rangle(t) = \frac{1}{n}\sum_{i=1}^{\lfloor nt \rfloor} \mathrm{Cov}_{i-1}(\zeta_n(i), \xi_n(i)) \xrightarrow{\mathbb{P}} \sigma^2 \int_0^t \frac{x(s)}{y(s)}\mathrm{d}s = \int_0^t \rho(s) \times \sigma\sqrt{\beta(s)}\mathrm{d}s.$$

From the martingale functional central limit theorem, we get that $(\bar{\boldsymbol{M}}_n^X, \bar{\boldsymbol{M}}_n^Y) \xrightarrow{d} (\hat{\boldsymbol{W}}_1, \hat{\boldsymbol{W}}_2)$, where $(\hat{\boldsymbol{W}}_1, \hat{\boldsymbol{W}}_2)$ are Brownian motions with zero means and quadratic covariation matrix

$$\begin{bmatrix} \int_0^t \beta(s)\mathrm{d}s & \int_0^t \rho(s) \times \sigma\sqrt{\beta(s)}\mathrm{d}s \\ \int_0^t \rho(s) \times \sigma\sqrt{\beta(s)}\mathrm{d}s & \sigma^2 t \end{bmatrix}.$$

The proof then follows by noting the fact that $(\boldsymbol{W}_1, \boldsymbol{W}_2) \overset{\mathrm{d}}{=\!=} (\hat{\boldsymbol{W}}_1, \hat{\boldsymbol{W}}_2)$. □

Having proved the above convergence of martingales, we now establish weak convergence of the scaled exploration process to a suitable diffusion process.

Proposition 7 (Functional CLT of the exploration process)**.** *As $n \to \infty$, $(\bar{\boldsymbol{X}}_n, \bar{\boldsymbol{Y}}_n) \xrightarrow{d} (\boldsymbol{X}, \boldsymbol{Y})$ where $(\boldsymbol{X}, \boldsymbol{Y})$ is the two-dimensional stochastic process satisfying the* SDE

$$\begin{aligned} \mathrm{d}X(t) &= \sqrt{\beta(t)}\left[\rho(t)\mathrm{d}B_1(t) + \sqrt{1-\rho(t)^2}\mathrm{d}B_2(t)\right] + f(t)X(t)\mathrm{d}t + g(t)Y(t)\mathrm{d}t, \\ \mathrm{d}Y(t) &= \sigma\mathrm{d}B_1(t), \end{aligned} \tag{A46}$$

with $\boldsymbol{B}_1$, $\boldsymbol{B}_2$ being independent standard Brownian motions, and $f(t)$, $g(t)$ and $\rho(t)$ as defined in (A4)*.*

Proof. First we show that $((\bar{\boldsymbol{X}}_n, \bar{\boldsymbol{Y}}_n))_{n\geq 1}$ is a stochastically bounded sequence of processes. Indeed stochastic boundedness (and in fact weak convergence) of the $\bar{\boldsymbol{Y}}_n$ process follows from Lemma 6. Further observe that for any $T < 1/\mu$, by Proposition 5,

$$\sup_{t\leq T}|f_n(t) - f(t)| \xrightarrow{\mathbb{P}} 0, \qquad \sup_{t\leq T}|g_n(t) - g(t)| \xrightarrow{\mathbb{P}} 0, \tag{A47}$$

where f, g are defined in (A4). Therefore, for any $T < 1/\mu$,

$$\sup_{t\leq T}|\bar{X}_n(t)| \leq \sup_{t\leq T}|\bar{M}_n^X(t)| + T\sup_{t\leq T}|g_n(t)\bar{Y}_n(t)| + \sup_{t\leq T}|f_n(t)|\int_0^T \sup_{u\leq t}|\bar{X}_n(u)|\mathrm{d}t,$$

and again using Grőnwall's inequality, it follows that

$$\sup_{t\leq T}|\bar{X}_n(t)| \leq \Big(\sup_{t\leq T}|\bar{M}_n^X(t)| + T\sup_{t\leq T}|g_n(t)\bar{Y}_n(t)|\Big) \times \exp\Big(T\sup_{t\leq T}|f_n(t)|\Big).$$

Then stochastic boundedness of $(\bar{\boldsymbol{X}}_n)_{n\geq 1}$ follows from Lemma 6, (A47), and the stochastic boundedness criterion for square-integrable martingales given in [48, Lemma 5.8].

From stochastic boundedness of the processes we can claim that any sequence $(n_k)_{k\geq 1}$ has a further subsequence $(n'_k)_{k\geq 1} \subseteq (n_k)_{k\geq 1}$ such that

$$(\bar{\boldsymbol{X}}_{n'_k}, \bar{\boldsymbol{Y}}_{n'_k}) \xrightarrow{d} (\boldsymbol{X}', \boldsymbol{Y}'), \tag{A48}$$

along that subsequence, where the limit $(\boldsymbol{X}', \boldsymbol{Y}')$ may depend on the subsequence $(n_k)_{k\geq 1}$. However, due to the convergence result in Lemma 6 and (A47), the continuous mapping theorem (see [49, Section 3.4]) implies that the limit $(\boldsymbol{X}', \boldsymbol{Y}')$ must satisfy (A46). Again, the solution to the SDE in (A46) is unique, and therefore the limit $(\boldsymbol{X}', \boldsymbol{Y}')$ does not depend on the subsequence $(n_k)_{k\geq 1}$. Thus, the proof is complete. □

Proof of Theorem 2. First observe that

$$\sqrt{n}(\hat{J}_n - \hat{J}) \xrightarrow{d} X(\hat{J}) \quad \text{as} \quad n \to \infty.$$

Indeed this can be seen by the application of the hitting time distribution theorem in [47, Theorem 4.1], and noting the fact that $x'(\hat{J}) = -1$. Now since $\mathbf{X}$ is a centered Gaussian process, in order to complete the proof of Theorem 2, we only need to compute $\mathrm{Var}(X(\hat{J}))$. We will use the following known result [50, Theorem 8.5.5] to calculate the variance of $X(t)$.

Lemma 8 (Expectation and variance of SDE)**.** *Consider the d-dimensional* SDE *given by*

$$\mathrm{d}Z(t) = (A(t)Z(t) + a(t))\mathrm{d}t + \sum_{i=1}^{d} b_i(t)\mathrm{d}B_i(t), \tag{A49}$$

where $Z(0) = z_0 \in \mathbb{R}^d$, the b_i's are $\mathbb{R}^d$-valued functions, and the B_i's are independent standard Brownian motions, $i = 1, \ldots, d$. Then given $Z(0) = x_0$, $Z(t)$ has a normal distribution with mean vector $m(t)$ and covariance matrix $V(t)$, where $m(t)$ and $V(t)$ satisfy the recursion relations

$$\frac{\mathrm{d}}{\mathrm{d}t}m(t) = A(t)m(t) + a(t), \quad \frac{\mathrm{d}}{\mathrm{d}t}V(t) = A(t)V(t) + V(t)A^T(t) + \sum_{i=1}^{d} b_i b_i(t)^T, \tag{A50}$$

with initial conditions $m(0) = x_0$ and $V(0) = 0$.

In our case, observe from (A46) that

$$\begin{aligned} A(t) &= \begin{bmatrix} f(t) & g(t) \\ 0 & 0 \end{bmatrix}, \quad a(t) = \begin{bmatrix} 0 \\ 0 \end{bmatrix}, \\ b_1(t) &= \begin{bmatrix} \rho(t)\sqrt{\beta(t)} \\ \sigma \end{bmatrix}, \quad b_2(t) = \begin{bmatrix} \sqrt{1-\rho(t)^2}\sqrt{\beta(t)} \\ 0 \end{bmatrix}. \end{aligned} \tag{A51}$$

Denote the variance-covariance matrix of $(X(t), Y(t))$ by

$$V(t) = \begin{bmatrix} \sigma_{xx}(t) & \sigma_{xy}(t) \\ \sigma_{xy}(t) & \sigma_{yy}(t) \end{bmatrix}. \tag{A52}$$

Then

$$\begin{aligned} \frac{\mathrm{d}}{\mathrm{d}t}V(t) &= \begin{bmatrix} \sigma_{xx}(t)f(t) + \sigma_{xy}(t)g(t) & \sigma_{xy}(t)f(t) + \sigma_{yy}(t)g(t) \\ 0 & 0 \end{bmatrix} + \begin{bmatrix} \sigma_{xx}(t)f(t) + \sigma_{xy}(t)g(t) & 0 \\ \sigma_{xy}(t)f(t) + \sigma_{yy}(t)g(t) & 0 \end{bmatrix} \\ &\quad + \begin{bmatrix} \rho(t)^2\beta(t) & \sqrt{\beta(t)}\sigma\rho(t) \\ \sqrt{\beta(t)}\sigma\rho(t) & \sigma^2 \end{bmatrix} + \begin{bmatrix} (1-\rho(t)^2)\beta(t) & 0 \\ 0 & 0 \end{bmatrix} \\ &= \begin{bmatrix} 2\sigma_{xx}(t)f(t) + 2\sigma_{xy}(t)g(t) & \sigma_{xy}(t)f(t) + \sigma_{yy}(t)g(t) \\ \sigma_{xy}(t)f(t) + \sigma_{yy}(t)g(t) & 0 \end{bmatrix} + \begin{bmatrix} \beta(t) & \sqrt{\beta(t)}\sigma\rho(t) \\ \sqrt{\beta(t)}\sigma\rho(t) & \sigma^2 \end{bmatrix}. \end{aligned}$$

Therefore, the variance of $X(t)$ can be obtained from the solution of the recursion equations

$$\begin{aligned} \frac{\mathrm{d}\sigma_{xx}(t)}{\mathrm{d}t} &= 2(\sigma_{xx}(t)f(t) + \sigma_{xy}(t)g(t)) + \beta(t), \\ \frac{\mathrm{d}\sigma_{xy}(t)}{\mathrm{d}t} &= \sigma_{xy}(t)f(t) + \sigma_{yy}(t)g(t) + \sqrt{\beta(t)}\sigma\rho(t), \end{aligned} \tag{A53}$$

and the proof is thus completed by noting that $\sigma_{yy}(t) = \sigma^2 t$. □

Appendix B: Simulation and comparison with Random Geometric Graphs

Fig. 7 confirms that the asymptotic analytical variance given in (A3) and (A4) is a sharp approximation for the CRG model with only 2000 vertices. Table II shows numerical values of $\hat{V}(c, \alpha_d)$ and compares the analytically obtained values of $\hat{J}(c, \alpha_d)$ and $\hat{V}(c, \alpha_d)$, and simulated mean and variance for the random geometric graph ensemble. The agreement again confirms the appropriateness of the CRG(c, α_d) model for modeling the continuum RSA. Furthermore, $\hat{V}(c, \alpha_d)$ serves as an approximation for the value of $V(c, d)$, the asymptotic variance of $J(c, d)$ (suitably rescaled). Fig. 8 shows the density function of the random variable based on the Gaussian approximation in Theorem 2. We observe that both the mean and the fluctuations around the mean decrease with c. Indeed, the variance-to-mean ratio has been typically observed to be smaller than one for RSA in the continuum, and it is generally believed that disordered packings are typically of sub-Poissonian nature with fluctuations that are not as large as for a Poisson distribution; see for instance the Mandel Q parameter in quantum physics [41]. So, while a closed-form expression remains out of reach (as for the Mandel Q parameter [41]), our solvable model gives a way to describe accurately the variance-to-mean ratio as $\hat{V}(c, \alpha_d)/\hat{J}(c, \alpha_d)$.

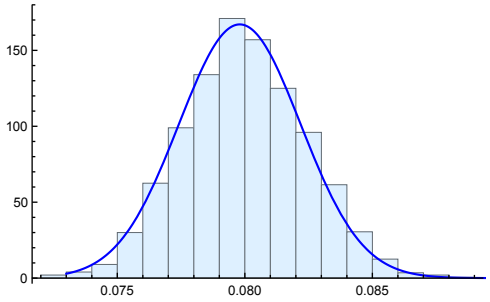

FIG. 7. Fitted normal curve for 2000 repetitions of the CRG$(20, \alpha_2)$ model with 1000 vertices. The solid curve represents the normal density with properly scaled theoretical variance $\hat{V}(c, \alpha_2)$, centered around the sample mean.

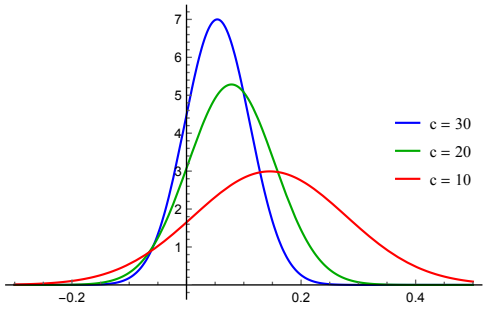

FIG. 8. Fitted normal curves for the CRG(c, α_2) model for increasing c values 10, 20 and 30. As c increases, the curve become more sub-Poissonian.

Appendix C: Clustering coefficient of Random Geometric Graphs

The goal of this section is to derive the (local) clustering coefficient for RGG(c, d). Consider n uniformly chosen points on a d-dimensional box $[0, 1]^d$ and connect two points u, v by an edge if they are at most $2r$ distance apart. Fix any three vertex indices u, v, and w. We write $u \leftrightarrow v$ to denote that u and v share an edge. The clustering coefficient for RGG(c, d) on n vertices is then defined by

$$C_n(c, d) := \mathbb{P}\left(v \leftrightarrow w | u \leftrightarrow v, u \leftrightarrow w\right). \tag{C1}$$

The following theorem explicitly characterizes the asymptotic value of $C_n(c, d)$.

		RGG		CRG	
n	c	$J_n(c, 2)$	$V_n(c, 2)$	$\hat{J}(c, \alpha_2)$	$\hat{V}(c, \alpha_2)$
200	10	0.1618	0.0166		
500	10	0.1608	0.0158	0.1454	0.0178
1000	10	0.1623	0.0155		
200	20	0.0887	0.0062		
500	20	0.0892	0.0068	0.0786	0.0057
1000	20	0.0890	0.0067		
200	30	0.0619	0.0039		
500	30	0.0620	0.0041	0.0538	0.0032
1000	30	0.0615	0.0043		

TABLE II. Comparison between the observed mean and scaled variance $n\text{Var}(J_n(c, 2))$ for the RGG model, and the theoretical mean and variance from Theorem 2 in dimension 2. The sample means and variances for the RGG model are calculated over 150 samples.

Theorem 9. *For any fixed $c > 0$, and $d \geq 1$, as $n \to \infty$,*

$$C_n(c,d) \to C(d) = d \int_0^1 x^{d-1} I_{1-\frac{x^2}{4}}\Big(\frac{d+1}{2}, \frac{1}{2}\Big)\, \mathrm{d}x.$$

Remark 10. In order for Theorem 9 to hold we do not need the average degree c to be some constant value. It remains true as long as the average degree is $o(n)$. We only need to assume that $r_n \to 0$ as $n \to \infty$, so that for large enough n, the $2r_n$ neighborhood of a uniformly chosen point is inside $[0,1]^d$, with high probability. That is why we suppress the subscript n below, and assume r to be sufficiently small.

Remark 11. It is worthwhile to note that the clustering coefficient is only a function of the dimension, and does not depend on the density parameter. Intuitively, this is because the asymptotic local clustering coefficient at any vertex u can be thought as the ratio of the number of triangles u is part of, and the number of wedges centered at u. In theRGG model, as the density parameter changes, both the numerator and denominator change in proportionally.

We now prove Theorem 9. Observe that the RGG model can be constructed by throwing points sequentially at uniformly chosen locations independently, and then connecting to the previous vertices that are at most $2r$ distance away. Since the locations of the vertices are chosen independently, without loss of generality we assume that in the construction of theRGG model, the locations of u, v, w are chosen in this respective order. Now, the event $\{u \leftrightarrow v, u \leftrightarrow w, v \leftrightarrow w\}$ occurs if and only if v falls within the $2r$ neighborhood of u and w falls within the intersection region of two spheres of radius $2r$, centered at u and v, respectively. Let $B_d(\boldsymbol{x}, 2r)$ denote the d-dimensional sphere with radius $2r$, centered at $\boldsymbol{x}$, and let $V_d(2r)$ denote its volume. Since r is sufficiently small, so that $B_d(\boldsymbol{x}, 2r) \subseteq [0,1]^d$, using translation invariance, we assume that the location of u is $\mathbf{0}$. Let $\boldsymbol{v}, \boldsymbol{w}$ denote the positions in the d-dimensional space, of vertices v and w, respectively. Notice that, conditional on the event $\{\boldsymbol{v} \in B_d(\mathbf{0}, 2r)\}$, the position $\boldsymbol{v}$ is uniformly distributed over $B_d(\mathbf{0}, 2r)$. Let $\boldsymbol{V}$ be a point chosen uniformly from $B_d(\mathbf{0}, 2r)$. Then the above discussion yields

$$\begin{aligned} C &= \frac{\mathbb{P}\left(u \leftrightarrow v, u \leftrightarrow w, v \leftrightarrow w\right)}{\mathbb{P}\left(u \leftrightarrow v, u \leftrightarrow w\right)} && \text{(C2)} \\ &= \frac{1}{(V_d(2r))^2} \int_{\boldsymbol{v} \in B_d(\mathbf{0}, 2r)} \mathbb{P}\left(\boldsymbol{w} \in B_d(\mathbf{0}, 2r) \cap B_d(\boldsymbol{v}, 2r)\right) \mathrm{d}\boldsymbol{v} \\ &= \frac{1}{V_d(2r)} \mathbb{E}[|B_d(\mathbf{0}, 2r) \cap B_d(\boldsymbol{V}, 2r)|]. && \text{(C3)} \end{aligned}$$

We shall use the following lemma to compute the expectation term in (C2).

Lemma 12 ([51])**.** *For any $\boldsymbol{x}$ with $\|\boldsymbol{x}\| = \rho$, the intersection volume $|B_d(\mathbf{0}, 2r) \cap B_d(\boldsymbol{x}, 2r)|$ depends only on ρ and r, and is given by*

$$|B_d(\mathbf{0}, 2r) \cap B_d(\boldsymbol{x}, 2r)| = V_d(2r) \cdot I_{1-\frac{\rho^2}{16r^2}}\Big(\frac{d+1}{2}, \frac{1}{2}\Big), \tag{C4}$$

where $I_z(a,b)$ denotes the normalized incomplete beta integral, given by

$$I_z(a,b) = \frac{\int_0^z y^{a-1}(1-y)^{b-1}\mathrm{d}y}{\int_0^1 y^{a-1}(1-y)^{b-1}\mathrm{d}y}.$$

Observe that the Jacobian corresponding to the transformation from the Cartesian coordinates $(x_1, \ldots, x_d)$ to the Polar coordinates $(\rho, \theta, \phi_1, \ldots, \phi_{d-2})$, is given by

$$J_d(\rho, \theta, \phi_1, \ldots, \phi_{d-2}) = \rho^{d-1} \prod_{j=1}^{d-2} (\sin(\phi_j))^{d-1-j}. \tag{C5}$$

Thus, (C2) reduces to

$$\begin{aligned}
C &= \frac{1}{(V_d(2r))^2}\int_{\boldsymbol{x}\in B_d(\mathbf{0},2r)} |B_d(\mathbf{0},2r)\cap B_d(\boldsymbol{x},2r)|\mathrm{d}\boldsymbol{x} \\
&= \frac{1}{V_d(2r)}\int_{\|\boldsymbol{x}\|\le 2r} I_{1-\frac{\|\boldsymbol{x}\|^2}{16r^2}}\Big(\frac{d+1}{2},\frac{1}{2}\Big)\mathrm{d}\boldsymbol{x} \\
&= \frac{1}{V_d(2r)}\int_0^{2r}\int_0^{2\pi}\int_0^{\pi}\cdots\int_0^{\pi}\rho^{d-1}I_{1-\frac{\rho^2}{16r^2}}\Big(\frac{d+1}{2},\frac{1}{2}\Big)\prod_{j=1}^{d-2}(\sin(\phi_j))^{d-1-j}\prod_{j=1}^{d-2}\mathrm{d}\phi_j\mathrm{d}\theta\mathrm{d}\rho \\
&= \Big(\int_0^{2r}\rho^{d-1}\mathrm{d}\rho\Big)^{-1}\int_0^{2r}\rho^{d-1}I_{1-\frac{\rho^2}{16r^2}}\Big(\frac{d+1}{2},\frac{1}{2}\Big)\mathrm{d}\rho,
\end{aligned}$$

since

$$V_d(2r) = 2\pi\Big(\prod_{j=1}^{d-2}\int_0^{\pi}(\sin(\phi_j))^{d-1-j}\mathrm{d}\phi_j\Big)\int_0^{2r}\rho^{d-1}\mathrm{d}\rho.$$

Therefore, putting $x=\rho/2r$, yields

$$C = \Big(\int_0^1 x^{d-1}\mathrm{d}x\Big)^{-1}\int_0^1 x^{d-1}I_{1-\frac{x^2}{4}}(\frac{d+1}{2},\frac{1}{2})\mathrm{d}x = d\int_0^1 x^{d-1}I_{1-\frac{x^2}{4}}(\frac{d+1}{2},\frac{1}{2})\mathrm{d}x. \tag{C6}$$